J. Water Environ. Nanotechnol., 8(3): 267-284 Summer 2023

ORIGINAL RESEARCH PAPER

Energy matrices and life cycle conversion analysis of N-identical hybrid double slope solar distiller unit using Al_2O_3 nanoparticle

Dharamveer Singh* [1,2], Ashok Kumar Yadav[3], Anil Kumar[4], Samsher[4,5]

[1]*Department of Mechanical Engineering, R. D Engineering College, Ghaziabad, U.P., India*
[2]*Research Centre, M. R. D. Trust, Modinagar, Ghaziabad, U.P., India*
[3]*Department of Mechanical Engineering, Raj Kumar Goel in stitute of technology, Ghaziabad, U P. india*
[4]*Department of Mechanical Engineering, Delhi Technological University, Delhi, India*
[5]*Department of Mechanical Engineering, H. B. T. U., Kanpur, U. P., India*

Received: 2023-02-19 Accepted: 2023-04-24 Published: 2023-08-10

ABSTRACT

In the current study, 25% incorporating PVT hybrid CPC collector double slope solar still is using Al_2O_3 nanoparticles underwent energy matrices analysis and life cycle conversion efficiency (LCCE). With the aid of an analytical program fed into MATLAB, the analysis is conducted on an annual basis based on the atmospheric conditions in New Delhi. The IMD in Pune, India, provided weather input data needed for the numerical computations. The average annual energy output will be calculated using energy and exergy and later on evaluated EPT, EPF, and LCCE. This will reveal that the average annual yield is 8.5%, the average energy payback time is 16.16%, the average energy payback factor is 13.91%, and the average life cycle cost conversion efficiency is 7.15% higher compared to the previous research. Therefore, it is obvious the proposed system is better based on the following parameters i.e. (i). annual yield, (ii). energy matrices such as EPT, EPF, and efficiency of life cycle cost (LCCE). The proposed hybrid is a self-sustainable system that can also meet the future requirements of potable water as well as electricity.

Keywords: Energy matrices, Energy payback time, Energy production factor, Life cycle conversion efficiency, Al_2O_3 nanoparticles

How to cite this article

Singh D., Kumar Yadav A., Kumar A., Samsher., Energy matrices and life cycle conversion analysis of N-identical hybrid double slope solar distiller unit using Al_2O_3 nanoparticle". J. Water Environ. Nanotechnol., 2023; 8(3): 267-284.
DOI: 10.22090/jwent.2023.03.006

INTRODUCTION

We can access a very low percentage of water from the ground. Therefore, there is a need to develop potable water and self-sustainable systems. Water purification is required due to polluted water to freshwater throughout the world. Consumption of polluted water is increasing death rates by increasing diseases in human beings. In present days, system availability is not self-sustainable. Electricity is needed which generates it causes pollution. Therefore, the better solution is a renewable energy source that can reduce the potable water problem. Lawrence and Tiwari [1] developed the empirical relations for the inside coefficients of heat transfer from the natural flow with a heat exchanger in a solar distiller unit. Popiel and Wojtkowiak [2] studied the thermo-physical properties of the base fluid. Pak and Cho [3] evaluated various correlations for different properties. G. N. Tiwari [4] studied the fundamental design of the solar still. Hwang et al. [5] analyzed the heat transfer coefficient for Al_2O_3 nanofluids.

* Corresponding Authors Email: *veerdharam76gmail.com*

Barden [6] improved the thermo-physical properties of the base fluid; the heat transfer coefficients could also be improved. Due to their superior thermo-physical characteristics, nanoparticles are easily deferred. The nanofluids are developing fluids with extremely quick heat transfer properties. Additionally, the base fluid's qualities could be enhanced by customizing the size and shape. Tiwari and Tiwari [7] expressed few merits of solar distillers over other distillation technologies such as filters, membranes, and batteries, no definitive resource of energy, and primarily low investment. Ho et al. [8] numerically analyzed nanofluids for natural convection in a square enclosure: effects due to uncertainties of viscosity and thermal conductivity. Otanicar and Golden [9] analyzed the enviro economic aspect of solar collectors using nanofluid and found it neutralizes 74 kg for a life span of 15 years. Patel et al. [10] found the thermal conductivity of nanofluids. Singh et al. [11] theoretically investigated entropy generation for nanofluids. Elzen et al. [12] analyzed emission reductions, abatement costs, and carbon prices. Khanafer and Vafai [13] This work presented the thermophysical properties of nanofluids. Khullar and Tyagi [14] analyzed and reported emissions of 103 kg approx./household/year reduced for a solar heating device for nanofluids. Faizel et al. [15] analyzed based on the cost of flat plate collector (FPC) using tin oxide, copper oxide, titanium oxide, and aluminum oxide) nanofluids. It is discovered that the high density, low specific heat, and thermal conductivity of CuO nanofluid are more appropriately attributed to its performance.Liu et al. [16] have evaluated the economic analysis of the integrated solar distiller unit of the evacuated tube. Kabeel et al. [17] analyzed the sole inclined solar distiller unit with vacuum as a water-based nanofluid. Elango et al. [18] analyzed practically single-slope solar distillers as thermal energy, exergy, and productivity using different nanofluids. Omara et al. [19] analyzed the performance of corrugated wick type and simple solar distiller units using nanofluids. Tiwari et al. [20] analyzed experimentally active solar distillers that exergoeconomic and environmental economic using water-based nanofluid the photovoltaic thermal flat plate collector is met potable water requirements daily. Environmental damage has been estimated to cost $6.29 annually. Sharon and Reddy [21] analyzed the annual economic performance of an active solar distiller loaded with saline water. Sahota et al. [22, 24] analyzed the passive double slope solar distiller unit performance using nanofluids and concluded that the aluminum oxide-based nanofluid gives better performance than others. Singh et al. [23] analyzed the energy matrix and existence cycle conversion efficiency for conventional single and double slope distiller units and found 0.144. and 0.137 per unit cost, respectively, and exergoeconomic parameters. Singh and Tiwari [25] analyzed the energy matrices and life cycle cost of an active partly PVT-CPC solar distiller. Shashir et al. [26] analyzed the performance of nanoparticles like copper oxide and graphite micro-flakes on solar distiller units with different cooling on the cover of toughened glass. It is concluded the solar yield increases and copper oxide 47.8% and 57.6%. Sahota et al. [27] studied the performance of PVT-FPC double slope solar distiller unit with or without helical coil heat exchanger using nanofluid and found water-based nanofluid performance was better with a heat exchanger. Saleha et al. [28] analyzed the effect of solvent and found it effective in solar distiller units. Chen et al. [29] analyzed that experimentally found the stability of weak luminous was very good with nanofluid in solar distiller unit and the effect of brackish water's constancy, ocular and thermal properties using nanofluid feasible. Mahian et al. [30] studied and found a significant temperature lower than 50 °C, in a heat exchanger and found a 2 times greater amount of water than without a heat exchanger. Additionally, water nanoparticles improve evaporation at low temperatures. It is crucial to assess the cost-effectiveness of renewable energy systems based on payback. Sahota et al. [31] analyzed environmental economics and exergoeconomics for passive double slope solar distiller with water-loaded nanofluid (CuO,Al_2O_3,TiO_2) and found payback time of energy of the system is low and the cost of environmental per annum is higher on mitigation with nanofluid. Singh and Tiwari [32] analyzed the augmentation in energy matrices of N-PVT-FPC partly double slope solar distiller. Joshi and Tiwari[33] analyzed single slope N^{th}-identical photovoltaic thermal compound parabolic concentrator collector N-PVT-CPC. Dharamveer et al. [34] reviewed nanofluid-loaded desalination. Kumar and Singh [35] analyzed the Energy and exergy of active solar stills using a compound parabolic concentrator. Shanker, et al.[36] analyzed the performance of the C.I. engine using biodiesel fuel by modifying injection timing and injection pressure Anup et al. [37] analyzed using FEA of refrigerator compartment for optimizing thermal efficiency. Kumar and Singh.[38]optimized thermal behavior of a small heat exchanger. Zhang et al. [39] presented in the area of sustainable energies focuses on utilizing green and clean technologies. Dhivagar et al. [40] analyzed single slope grate crude shrewd solar distiller units for energy, exergy, and economic aspects. Dharamveer and Samsher [41] studied the active and passive solar still behavior on energy matrices and enviroeconomics. Arora et al. [42] analyzed double slope solar distiller N-PVT-CPC using carbon nanotubes for water generation. Dharamveer et al. [43] analytically studied N^{th} identical photovoltaic thermal (PVT) compound parabolic concentrator (CPC) active double slope solar distiller with a helically coiled heat exchanger using C_uO Nanoparticles. Dharamveer, et al. [44] analyzed an N-identical active single-slope solar distiller with a helically coiled heat exchanger using CuO nanoparticles. Kumar and Singh, [45] compared single-phase microchannels for heat flow Experimental and using CFD. Subrit and Singh. [46] analyzed thermal of coal and waste cotton oil liquid produced by pyrolysis of diesel engine fuel was carried out by. Shahsavar et al. [47] Compared energy, exergy, environmental, exergoeconomic, and enviro economic analysis of building integrated photovoltaic/thermal, earth-air heat exchanger, and hybrid systems. Numerous studies on passive and active solar stills have been conducted, according to the current literature survey. However, not much investigation on active solar still filled with water-based nanofluids was studied. Based on energy and exergy, Dharamveer et al. studied a hybrid double slope. No scholars have examined the economic, and environmental, using nanofluid. Furthermore, no studies have been conducted for CPC, ETC double slope basin type solar distiller using nanofluid. Thus, the proposed study will examine the impacts of active solar still double slope with CPC and filled with water containing Al_2O_3 nanofluid on energy matrices based such as energy payback time, energy payback factor, life cycle cost conversion efficiency, and productivity, of solar desalination systems will be thoroughly examined. The effectiveness of the suggested approach will also be evaluated in comparison to the findings of past studies.

MATERIALS AND METHODS

To determine the following objectives the methodology is adopted as energy matrices analysis of hybrid solar distiller basin type double slope with heat exchanger using Al_2O_3 nanoparticles.

System Description

Working of double slope solar desalination incorporating PVT with CPC collector using nanoparticles (N-PVT-CPC-DS-HE) is shown. Representation of solar still is followed the greenhouse principle. The parameters used for the distiller unit are given in Table 1 and Table 2. The basin of the solar distiller is connected in series with N-CPC and incorporated with a helically coiled heat exchanger. Solar radiation received on the glass cover is transferred to the water surface and thereafter absorbed by the surface. Later on, reflected water received heat on the top cover and rest portion and then move to the liner where the maximum amount absorbed and liner temperature increased and transfer this heat to water. Thus the temperature of water in the basin is increased and water gets evaporated. Collectors also heat the water in the basin. Water is heated and evaporates in this manner. The distillate trickles forward to the passage attached to the bottom side as the vapor reaches the interior face of the condenser, where film-wise condensation takes place. Then, the beaker receives the distilled water that was siphoned off.

Fig. 1 represents 25% PVT incorporating hybrid solar still. Collectors are put south facing at an angle of 45º which are connected in series as the input of the second collector is attached to the first collector output. Radiation that falls on the collector directly gets absorbed and beam irradiation is reflected on the parabolic concentrator. Similarly, irradiation falls on PV modules that generate electricity which is further used for operating pumps (D.C) and access energy can be further used for any electrical appliances according to need. Table 2 represents the specifications of the proposed system. The inclination angle of the system is 30º and the orientation of the system is the southern face. The basin liner is absorbed maximum radiation which falls on the glass cover. The basin fluid gets heat from the heat exchanger through Al_2O_3 nanoparticles. As per a prior study, it is obvious that a helically coiled heat exchanger is more effective than any other design. The Al_2O_3 nanoparticles exchange more heat in active solar still because it covers more

Table 1. Specifications of double slope PVT-CPC-DS active solar distillation system [43]

Hybrid solar distiller unit	
Components	Particulars
Basin length	2.0 m
Basin width	1.0 m
Tilting glass cover	15°
Basin (smaller side) height	0.2 m
Body's material	G.R.P
Stand's material	G.I.
Covers	Glass
Collector facing	south
Tilting glass thickness	0.004 m
K_g	0.816 W/mK
Insulation width	0.1 m
Thermal conductivity of insulation	0.166 W/mK

Hybrid collector			
Component's name	Specifications	Component's name	Specifications
Kinds of collector	Tube kinds	Area of aperture	2 m^2
Receiver area	1.0 m^2	Aperture's module area	1.0 m^2
Collector's plate thick	0.0020 m	Aperture's receiver area	1.5 m^2
Copper's tube thick	0.00056 m	Module's receiver area	0.25 m^2
Copper's tube length	1.0 m	Collector's receiver area	0.75 m^2
Packing coefficient	0.8	No of collectors	N=4
D.C. motor	12V, 40 Watt	Pipe dia.	0.0125 m
Inclination of CPC	30°	Inclination of FPC	30°
Under glass effective area	0.75 m^2	Under PV module effective area	0.660 m^2
No. of the cell (solar)	36	Single-cell (Solar)	0.007 m^2
Basin area	2 m^2	m_f	0.02 kg/s

Heat exchanger (copper coiled)			
No. of turns	12	Tube coil dia	0.0125 m
Length of heat exchanger	1.937 m	Heat exchanger coil dia	0.045 m

Table 2. Parameters are used for calculations [43]

Specifications	Numerical values	Specifications	Numerical values
α_g	0.050	A_{am}	0.5
α_b	0.5861	A_{ac}	1.5
α_{bf}	0.82	L_p	0.0020
α_c	0.90	K_m	64 W/mK
α_p	0.80	K_p	64 W/mK
β_c	0.89	L_i	0.1m
K_g	0.8160 W/mK	h_i	5.7 W/m^{2}K
K_b	0.035 W/mK	h_0	9.5 W/m^{2}K
K_p	0.166 W/mK	U_{tcp}	5.5451 W/m^{2}K
L_g	0.004	U_{tca}	15.03 W/m^{2}K
L_c	0.005	U_{tpa}	5.56 W/m^{2}K
L_i	0.1	U_{Lm}	9.03 W/m^{2}K
β_0	0.0045/K	U_{LC}	5.43 W/m^{2}K
x	0.33m	PF_1	0.2695
σ	5.67*10^{-8} (W/m^2K^4)	PF_2	0.9398
τ_g	0.95	PF_c	0.977
$F^/$	0.968	ϵ_g	0.95
η_0	0.15	ϵ_{bf}	0.95

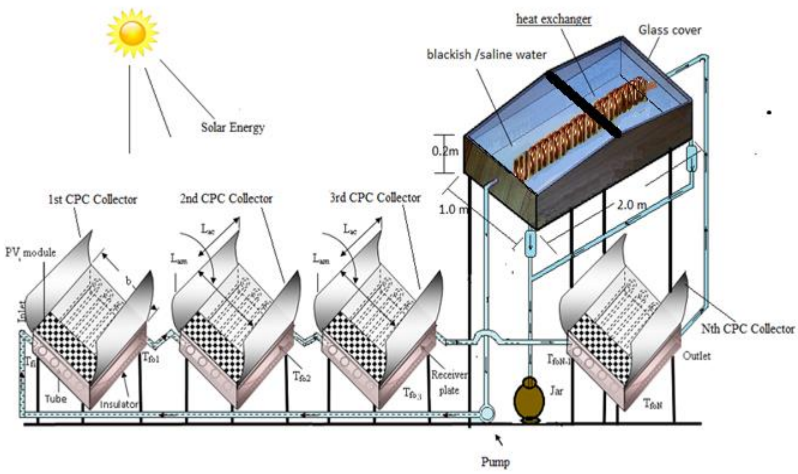

Fig. 1 active double slope solar still 25% incorporating N-PVT-CPC-DS-HE surface area due to increasing volume due to heat exchanger. The system gets thermal energy via a combination of double-slope basins incorporating with PVT-CPC collector unit and it absorbs heat externally from a collector and internally from a basin. Basin water temperature increases via heat exchanger nanoparticles. Ultimately by releasing latent heat the vapor gets condensed, and collected at the lower end of the inclined glass cover of the basin.

This sort of system produced electricity as well as potable water. The other quality of this sort of system is i.e. low maintenance, easy to install, and useful for large and small demands of potable water as well as industrial purpose. Lot of advantages of such a system but in this work, we emphasize producing potable water only therefore according to making the system self-sustainable the PVT is provided otherwise 50%, 75%, and 100% can also be used.

Though, the proposed system-A is compared with the previous System-B based on basin water temperature, inside glass cover temperature, water outlet temperature, the overall thermal energy of collectors, overall exergy, overall electrical exergy, and potable water amount. Sedimentation possibility in nanofluid is more. Therefore nanoparticles size leads to a change in aggregation. The value of size matters to change in aggregation. Later on, more sophisticated equipment is needed to remove it.

Governing equations

To develop the characteristic equation, the following assumptions are:

i. Constant water level
ii. Negelectedohmic losses
iii. No leakage
iv. Over the entire surface film condensation
v. Steady-state partially covered active solar stills

The governing equations of the system are as follows:

a. East face

$$\alpha_g I_{SE} A_{gE} + h_{1wE}(T_w - T_{giE})\frac{A_b}{2} - h_{EW}(T_{giE} - T_{giW})A_{gE} = U_{cgaE}(T_{giE} - T_a)A_i \quad (1)$$

b. West face

$$\alpha_g I_{SW} A_{gW} + h_{1wW}(T_w - T_{giW})\frac{A_b}{2} + h_{EW}(T_{giE} - T_{giW})A_{gW} = U_{cgaW}(T_{giW} - T_a)A_{gW} \quad (2)$$

On solving Equations (1) and (2)

$$T_{g\,iE} = \frac{A_1 + A_2 T_w}{P} \quad (3)$$

$$T_{g\,iW} = \frac{B_1 + B_2 T_w}{P} \quad (4)$$

$$T_{goE} = \frac{\frac{K_g}{L_g} T_{giE} + h_{1gE} T_a}{\frac{K_g}{L_g} + h_{1gE}} \quad (5)$$

$$T_{goW} = \frac{\frac{K_g}{L_g} T_{giW} + h_{1gW} T_a}{\frac{K_g}{L_g} + h_{1gW}} \quad (6)$$

The unknown terms, A_1, A_2, B_1, B_2, and P in Equations 3, 4, 5, and 6 are mentioned in Appendix A,

c. Basin liner

$$\alpha_b(I_{SE} + I_{SW}) + 2h_{bw}(T_b - T_w) + 2h_{ba}(T_b - T_a) \quad (7)$$

d. Water equation

$$m_f C_f \frac{dT_w}{d_t} = \alpha_w(I_{SE} + I_{SW})\frac{A_b}{2} + 2h_{bw}(T_b - T_w)\frac{A_b}{2} - h_{1wE}(T_w - T_{giE})\frac{A_b}{2} - h_{1wW}(T_w - T_{giW})\frac{A_b}{2} + Q_{uN} \quad (8)$$

e. Energy balance equations for heat exchange and base fluid can be written for solar distillers as:

$$m_f C_f \frac{dT_w}{d_x} d_x = -(2\pi r_{11} U)(T_{HE} - T_w) d_x \quad (9)$$

Applying the limits Tw at (x = 0) = T_{woN} and Tw at (x = L) = T_{wi} on solving,

$$T_{wi} = T_{HE}\left[1 - \exp\left(\frac{-(2\pi r_{11} UL)}{m_f C_f}\right)\right] + T_{woN} \exp\left(\frac{-(2\pi r_{11} UL)}{m_f C_f}\right) \quad (10)$$

Where $U = [\frac{1}{h_{bf}} + \left(\frac{r_{11}}{k_1}\right) \ln(\frac{r_{22}}{k_1})(\frac{1}{h_{bf}})]^{-1}$

f. Energy balance for water collector N-PVT-CPC

$$T_{woN} = \left[\frac{(AF_R(\alpha\tau))_1(1 - K_p^N)}{m_f C_f(1 - K_p)}\right] I_b + \left[\frac{(AF_R(UL)_1)(1 - K_p^N)}{m_f C_f(1 - K_p)}\right] T_a + T_{wi} K_m^N \quad (11)$$

$$T_{woN} = \left[\left[\frac{(AF_R(\alpha\tau))1(1 - K_p^N)}{m_f C_f(1 - K_p)}\right]\left(\frac{1}{(1 - e^z K_m^N)}\right)\right] I_b +$$

$$\left[\frac{(AF_R(UL)1)(1-K_p^N)}{m_f C_f(1-K_p)}\left(\frac{1}{(1-e^z K_m^N)}\right)\right] T_a +$$

$$T_{HE}\left(\frac{(1-e^z)K_m^N}{(1-e^z K_m^N)}\right)\Bigg] \quad (12)$$

Using this relation heat gain computed

$$Q_{uN} = m_f C_f\,(T_{woN} - T_{wi}) \quad (13)$$

The outlet temperature of water computed by these two equations 3.12 and 3.13,

$$T_{HE} > T_{wi} > T_w$$

$$Q_{uN} = [((\frac{(AF_R(\alpha\tau))1\,(1-K_p^N)}{(1-K_p)})\left(\frac{1}{(1-e^z K_m^N)}\right))I_b +$$

$$\left(\left(\frac{(AF_R(UL)1)(1-K_p^N)}{(1-K_p)}\right)\left(\frac{1}{(1-e^z K_m^N)}\right)\right) T_a +$$

$$m_f C_f\,(T_{HE}(\frac{(1-e^z)K_m^N}{(1-e^z K_m^N)}) - T_{wi})] \quad (14)$$

By putting

T_{giE}, T_{giW}, $2h_{bw}$ $(T_b$-$T_w)$, and Q_{uN} from Equations (3),(4), and (9) in Equation (15)

$$\frac{dT_w}{dt} = -a_2 T_w + f_2(t) \quad (15)$$

The energy and exergy analysis has been done, respectively, based on the thermodynamics laws for the given entities.

$$E_{hourlyEn} = [h_{1wE}(T_w - T_{giE}) + h_{1wW}(T_w - T_{giW})](A_b) \quad (16)$$

$$E_{hourlyEx} = \{h_{1wE}[(T_w - T_{g\,iE}) - (T_a + 273)\ \ln\left(\frac{T_w + 273}{T_{g\,iE} + 273}\right) + h_{1wW}[(T_w - T_{g\,iW}) - (T_a + 273)\ \ln\left(\frac{T_w+273}{T_{g\,iW}+273}\right)]\}A_b \quad (17)$$

The constant 0.933 represents the solar irradiation exchange constant, per hour water production for the proposed system have been calculated using the following equation.

$$M_w = \frac{q_{ew}}{L_v}3600 = \frac{h_{ew}(T_w - T_g)}{L_v}3600 \quad (18)$$

Latent heat of vaporization is expressed as [43]:

L_v=3.162510^6+[1-(7.61610^{-4} T_v)] For T_v> 70 °C

L_v=2.493510^6 [1-(9.477910^{-4} T_v)+1.313210^{-7} (T^2_v)-4.797410^{-3} (T^3_v)]

For T_v< 70 °C

Thermophysical properties of vapor, base fluid from references [31-34], and Nanoparticles (Table - 3) [37- 42].

Analysis based on matrices and cost conversion based on the life span of hybrid active double slope solar distiller unit using Al_2O_3 nanoparticles -

Energy matrices inform about the time of energy payback (EPT), energy payback factor (EPF), and life cycle conversion efficiency for the lifetime period (LCCE) [27].

Energy Payback Time (EPT) [27]

The time duration needed to recover total exhausted energy in manufacturing material can be expressed as

$$EPT_{(e)} = \frac{\text{Embodied Energy}(E_{in})}{\text{Annual energy output}(E_{out})} \quad (19)$$

$$EPT_{(ex)} = \frac{\text{Embodied Energy}(E_{in})}{\text{Annual exergy output}(E_{out})} \quad (20)$$

Energy Production Factor (EPF) [27]

It is reciprocal of EPT an ideal value of EPF on an annual basis to express the overall performance of solar still can be expressed as

$$EPF_{(e)} = \frac{\text{Overall Energy Output}(E_{out})}{\text{Embodied Energy}(E_{in})} \quad (21)$$

$$EPF_{(ex)} = \frac{\text{Overall Exergy Output}(E_{out})}{\text{Embodied Energy}(E_{in})} \quad (22)$$

Lifecycle Conversion Efficiency (LCCE) [27]

$$LCCE_{(e)} = \frac{E_{out} \times n - E_{in}}{E_{sol} \times n} \quad (23)$$

Where, E_{sol} represents annual solar energy (kWh) and n is the overall lifetime period.

Table 3. Thermophysical properties of Al2O3 nanoparticles [43]

Nanoparticles (NPs)	Density k_g/m^3	Thermal conductivity k_p (W/mK)	Specific heat C_p (j/k_g K)
Al_2O_3	$6.3*10^3$	17.6	550

Table 4. Daily, Monthly, and Annually yield of the proposed system

Month	whether condition type (a)			whether condition type (b)			whether condition type (c)			whether condition type (d)			Monthly yield
Jan	14.70	3	44.09	12.78	8	102.21	4.17	11	45.86	1.21	9	10.85	203.01
Feb	13.82	3	41.47	13.44	4	53.75	4.57	12	54.81	1.42	9	12.78	162.82
Mar	18.20	5	90.98	18.10	6	108.63	9.02	12	108.19	5.00	8	40.00	347.81
Apr	20.51	4	82.03	21.53	7	150.68	11.72	14	164.12	10.90	5	54.49	451.32
May	21.98	4	87.92	19.45	9	175.01	15.07	12	180.81	11.00	6	66.00	509.74
Jun	12.49	3	37.48	18.97	4	75.89	12.25	14	171.56	7.83	6	47.01	331.94
Jul	15.19	2	30.38	15.19	3	45.57	11.51	10	115.12	6.70	17	113.97	305.04
Aug	15.27	2	30.53	15.47	3	46.40	9.65	7	67.52	5.78	19	109.73	254.19
Sep	16.46	7	115.23	16.03	3	48.10	12.18	10	121.79	7.66	10	76.64	361.76
Oct	15.11	5	75.53	10.88	10	108.84	8.42	13	109.44	4.36	3	13.07	306.89
Nov	14.81	6	88.88	10.22	10	102.16	4.12	12	49.50	3.71	2	7.41	247.95
Dec	14.79	3	44.36	9.14	7	64.01	4.92	13	64.01	1.44	8	11.53	183.92
	Annual yield in (kg)												3666.39

Economic analysis is required to determine of hybrid active double slope solar still using Al_2O_3 nanoparticles-

It is economically feasible for System-A and System-B for both systems.

Capital cost

Tables 5 and 6 provide the system's fabrication cost.

System's Lifespan

It is considered for 15, 20, and 30 years.

Salvage value (S)

Salvage value (s) = 0.2 × Principal capital (PCC) (24)

PCC stands for principal capital cost

Cost of annual salvaging (ASC)

Annually salvage = S × shrinkage in a fund (SFF) (25)

SFF is a factor used for shrinkage

Yearly maintenance (AMC)

Yearly maintenance (AMC) =0.15×FAC (26)

FAC stands for the first annual cost.

Factor for capital recovery (CRF).

At a fixed rate of interest, it shows the present cost as a constant annual cost across time.

$$CRF = \frac{i(1+i)^n}{(1+i)^n - 1} \tag{27}$$

Shrinking fund factor

$$SFF = \frac{i}{(1+i)^n - 1} \tag{28}$$

Firstly annual cot estimated

FAC=PCC×CRF (29)

Net annual cost estimated

TAC= FAC+AMC-ASC (30)

Cost of distillate per kg obtained

$$Cost/kg = \frac{TAC}{\text{yield in life}} \tag{31}$$

Table 5. Embodied Energy of different components of system-A (N-PVT-DS-CPC-HE) and system-B (N-PVT-DS-FPC-HE)

Name of component	Embodied energy (kWh)	
	N-PVT-FPC-DS-HE (Previous system)[30]	N-PVT-CPC-DS-HE (Present system)
FRP body of DS	755.61	755.61
GI angle Iron	416.4	416.4
Glass cover	180.5	180.5
FPC (N=4)	2209.92	-
CPC (N=4)	-	3279.41
PV (glass-glass)	980	980
Copper heat exchanger	25.83	25.83
Nanoparticles (CuO)	17.82	17.82
Others	20	20
Total EE of system	4606.08	5675.57

Table 6. Capital investment and cost of different components of system-A (N-PVT-DS-CPC-HE) and system-B (N-PVT-DS-FPC-HE)

Parameters	N-PVT-FPC-DS-HE [32]		N-PVT-CPC-DS-HE	
	Cost	Previous system	Cost	Present system
	₹	$	₹	$
FRP body	10200	139.135	10200	139.135
Glass cover 2.05	1600	21.825	1600	21.825
Iron stand	1000	13.641	1000	13.641
Inlet /outlet nozzle	200	2.728	200	2.728
Iron clamp	250	3.410	250	3.410
Gaskets	200	2.728	200	2.728
Silicon gel	200	2.728	200	2.728
PVT-FPC (N=4) 8500	34000	463.784		0.000
PVT-CPC (N=4) 9000		0.000	36000	491.06
Motor and pump	1200	16.369	1200	16.369
Helically coiled heat exchanger	466.25	6.360	466.25	6.360
Fabrication and other cost	6000	81.844	6000	81.844
100 gmsAl_2O_3nanoparticles	7425	101.282	7425	101.282
Total cost of	62741.25	855.83	64741.25	883.11

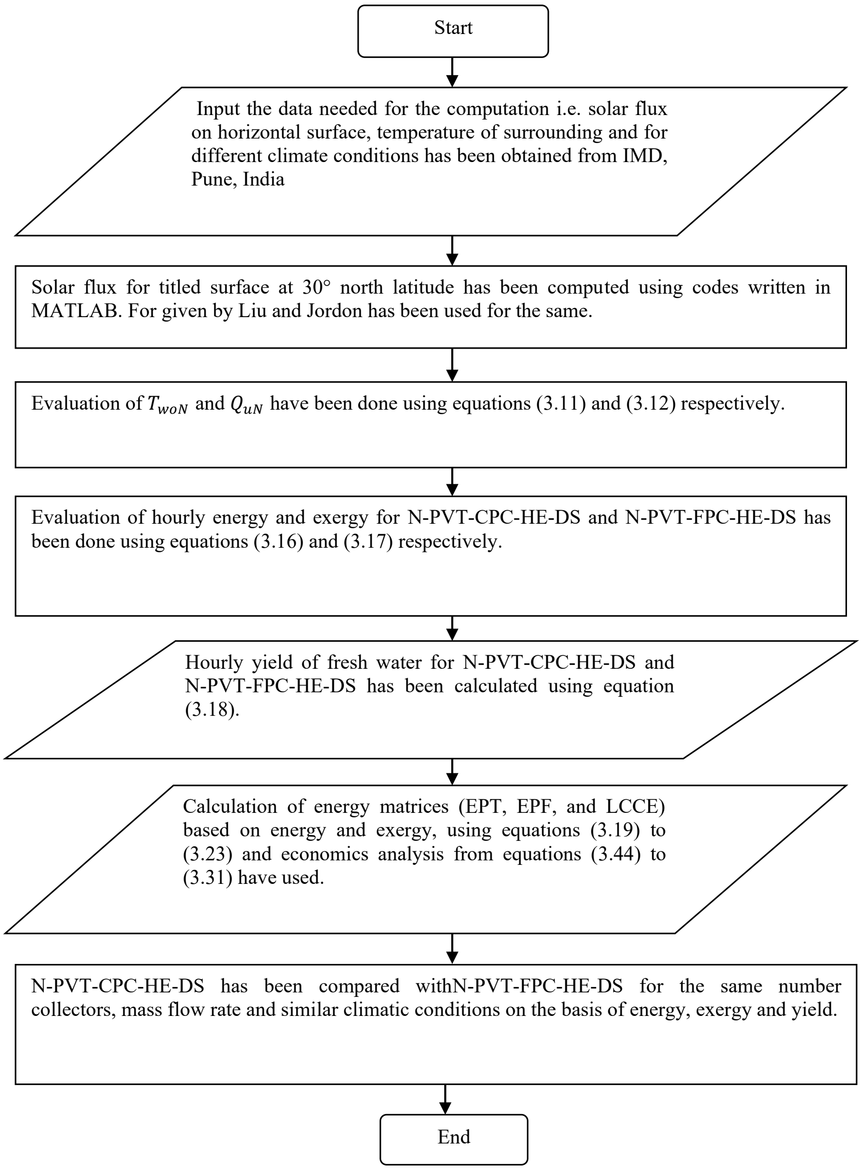

Fig. 2 Flow chart of the methodology adopted

Methodology to be Adopted

The following steps are included in the approach used to study the suggested system (Fig. 2):

Step-I

The proposed systems for the yearly are calculated using the Lui-Jordon formula for global and beam irradiation. Calculate daily solar radiation further by multiplying the number of days given in a month by the number of clear, hazy, hazy, cloudy, and cloudy days.

Step-II

The temperature of basin water is calculated based on hourly, monthly, and annual data, and all settings are tuned to maximize the collector's output temperature.

Step-III

Energy matrices such as efficiency of life cycle cost, Factor energy payback, energy payback time, and productivity have been evaluated.

Step-IV

Comparing proposed systems to the prior system using numerically computed values.

RESULT AND DISCUSSION

The solar irradiation on a flat area and surroundings temperature have been computed using

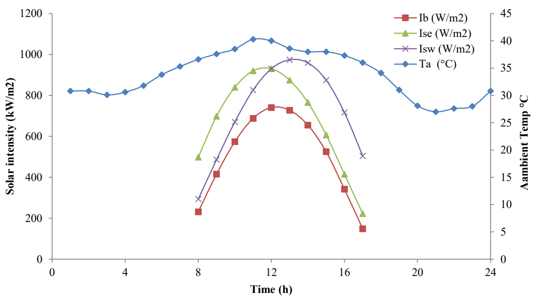

Fig. 3 Hourly variation in solar irradiation and ambient temperature for typical day of May

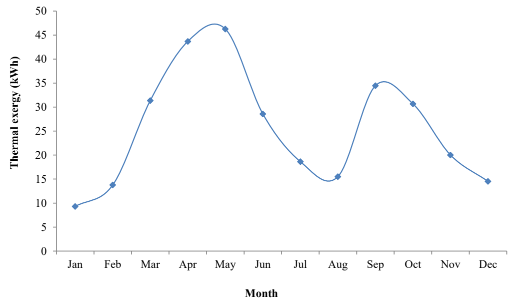

Fig. 4 Shows the thermal exergy of the proposed system-A

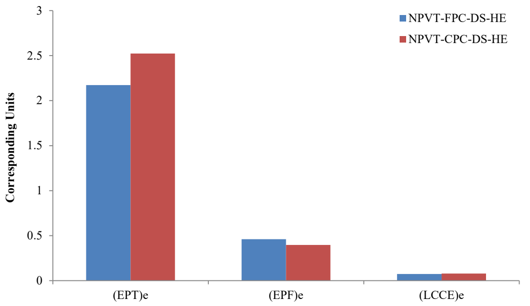

Fig. 5 Shows EPT, EPF, and LCCE for proposed and previous system for 15 years

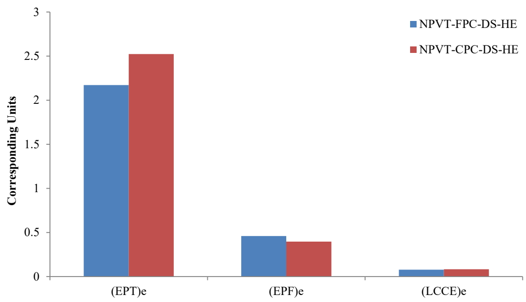

Fig. 6 Shows EPT, EPF, and LCCE for proposed and previous system for 20 years

IMD Pune data, India. By entering the pertinent data in MATLAB, the Liu and Jordan formula may be used to determine how much radiation was applied to N-PVT-CPCs. The values of beam radiation Ib, solar radiation Eastside ISE, Westside ISW, and ambient temperature Ta in kW/m^2 and °C, respectively, are shown in Fig. 3. Below Fig.4 shows a variation of the thermal exergy month-wise of proposed system-A.

Energy matrices and a life cycle cost conversion analysis are required for the hybrid active double slope solar distiller unit

Embodied energy (E_{in}), the conversion efficiency of the life cycle (LCCE), energy payback factor (EPF), and energy payback time for (N-PVT-DS-FPC-HE) and (N-PVT-DS-CPC-HE) are shown in Fig. 5, Fig. 6, and Fig. 7 for 15, 20 and 30 years respectively.

The number of energy matrices based on energy and exergy for proposed system-A is found that system-A is better to system-B. EPT based on energy and exergy is 16.16% and 17.84% higher, respectively. EPF based on energy and exergy is relatively less13.91% and 14.88%, respectively. LCCE based on energy and exergy is appreciably greater for system-A than system-B: 5.55%, 6.38%, and 7.15% for 15, 20, and 30 years of life considered, respectively.

Economic analysis is required to determine whether hybrid active solar still uses Nanoparticles (Al_2O_3)

It is economically feasible for system-A and System-B annually. Total yearly cost, fixed annual cost, yearly maintenance cost, and yearly water generation for system-A and system-B are shown during 30 years, at respective interest rates of 1%, 3%, and 5% respectively are represented in Fig. 8, and Fig. 9.

The cost of distillation relies on the rate of interest, as results over 30 years are shown in Fig.8. While the cost of distillate will reduce as system life increases, the price of distillate will climb annually as interest rates rise. For system-A and system-B, the cost of distillate is 0.69, 0.96, and 1.27 (/kg), and 0.72, 1.012, and 1.33 (/kg), respectively, over 30 years at interest rates of 1%, 3%, and 5%. According to the cost of distillation, it is concluded that the proposed system-A performs better than system B.

CONCLUSION AND FUTURE SCOPE

The proposed system and previous system performance have been studied using characteristic

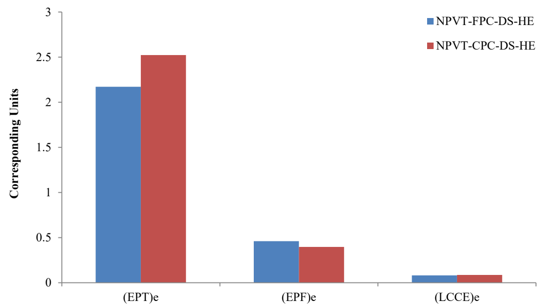

Fig. 7 Shows EPT, EPF, and LCCE for proposed and previous system for 30 years

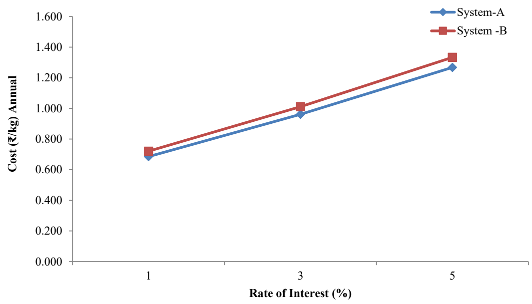

Fig. 8 Represents cost of distillate vs Interest rate

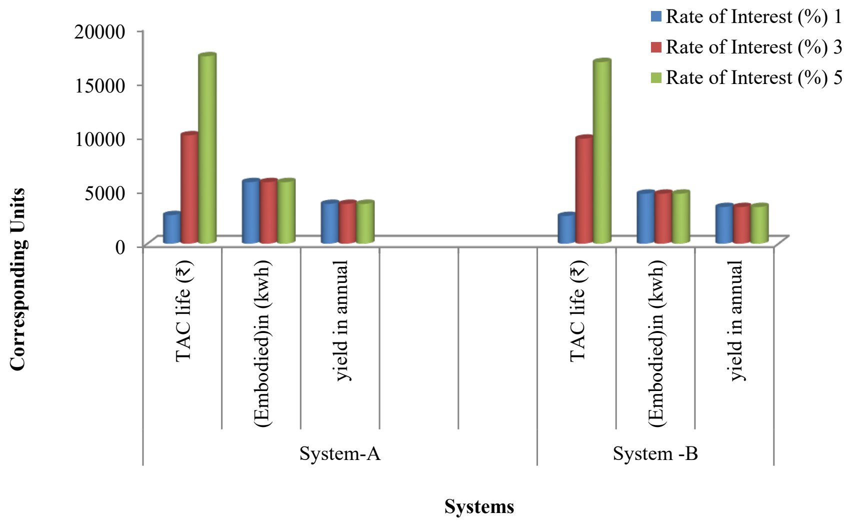

Fig. 9 Shows comparison for system-A and system-B based on TAC, Embodied Energy and Yield for 30 years

equations and Al_2O_3 nanoparticles and found better than the previous system.

Conclusions

The following conclusions are made by the annual analysis of the proposed systems with Al_2O_3 nanoparticles.

1. The proposed system-A gives better annual performance than system-B based on thermal exergy, energy, yield is 8.5%, and productivity 5.17% greater with Al_2O_3 nanoparticles.
2. Al_2O_3 nanoparticles-based system-A gives better results on annual performance and economics as compared to system-B.
3. Based on thermal energy, thermal exergy, energy, and exergy-based, Energy payback time (EPT) is 16.16%, Energy payback factor (EPF) is 13.91%, Efficiency of life cycle cost (LCCE) is 7.15% greater than the previous research, it is found that system-A outperforms system-B (previous).
4. System-A has a lower distillation cost than System B (previous). The yearly cost of distillate for systems A and B is 0.69, 0.96, and 1.27 (/kg), and 0.72, 1.012, and 1.33 (/kg), respectively, based on a 30-year basis at interest rates of 1%, 3%, and 5%. According to distillate cost, it is discovered that system-A performs better than system B.

Future scope

This work can be further expanded using research with PCM material in CPC up to a specific level.

1. Energy and exergy can be studied for different nanoparticles
2. energy matrices, EPT, EPF, and LCCE can be studied for different nanoparticles
3. Research on the environmental and economic benefits of various nanoparticles is possible. Different sizes, and shapes of nanoparticles can be investigated.
4. The partial covered 50%, 75%, and 100% can be studied.

Nomenclature

A_{ba} basin surface, in (m^2)
A_{ca} flat plate collector area under glazing, in (m^2)
A_{gE} eastside glass cover area, in (m^2)
A_{gW} westside glass cover area, in (m^2)
A_m PVT area, in (m^2)
C_p specific heat NPs, in (J/kgK)
C_{bf} base fluid specific heat, in (J/kgK)
C_{nf} specific heat nanofluid, in (J/kgK)
D_i FPC tube dia., in (m)
d_p Nps dia., in (nm)
F' the factor of collector efficiency
h_i coefficient of heat transfer glazing to absorbing plate, in $(W/m^2\,K)$
h_o heat transfer coefficient top of PVT to ambient air, in $(W/m^2\,K)$
h_{pw} heat transfer coefficient blackened plate to fluid, in $(W/m^2\,K)$
h_{bw} heat transfer coefficient liner to ambient, in $(W/m^2\,K)$
h_{ba} coefficient of heat transfer from basin to ambient, in $(W/m^2\,K)$
h_{CPC} coefficient of heat transfer convective in CPC, in $(W/m^2\,K)$
h_{HE} in heat exchanger convective heat transfer coefficient, in $(W/m^2\,K)$
h_{rwgE} eastside, water-to-glass heat transfer coefficient radiative, in $(W/m^2\,K)$
h_{rwgW} westside, water-to-glass heat transfer coefficient radiative, in $(W/m^2\,K)$
h_{cwgE} eastside, water-to-glass heat transfer coefficient radiative, convective in $(W/m^2\,K)$
h_{cwgW} westside, water-to-glass heat transfer coefficient radiative, convective in $(W/m^2\,K)$
h_{ewgE} eastside, water-to-glass heat transfer coefficient radiative, evaporative in $(W/m^2\,K)$
h_{ewgW} westside, water-to-glass heat transfer coefficient radiative, evaporative in $(W/m^2\,K)$
h_{1gE} eastside, coefficient of total heat transfer, in $(W/m^2\,K)$
h_{1gW} westside, coefficient of total heat transfer, in $(W/m^2\,K)$
h_{1wE} eastside water to glass cover coefficient of heat transfer, in $(W/m^2\,K)$
h_{1wW} westside water to glass cover coefficient of heat transfer, in $(W/m^2\,K)$
I_b on the collector solar irradiation, in (W/m^2)
I_{SE} eastside over-glass cover solar irradiation, in (W/m^2)
I_{SW} westside over glass cover solar irradiation, in (W/m^2)
K_g in glass heat conductivity$(W/m\,K)$
K_p in absorbing plate heat conductivity $(W/m\,K)$
k_p in nanoparticles, heat conductivity$(W/m\,K)$
K_{nf} in nanofluid heat conductivity $(W/m\,K)$
K_{bf} in base fluid heat conductivity$(W/m\,K)$
L length of heat exchanger coil, in (m)
L_c glazing length collector, in (m)
L_i the thickness of insulation, in (m)
L_g cover of glass thickness, in (m)
L_m length of PVT, in (m)
L_p absorbing plate thickness, in (m)
M_w water mass, in (k_g)
M_{ew} yield, in (k_g)
m_f water flow rate, in (k_g/s)
PF_1 penalty factor 1
PF_2 penalty factor 2
PF_3 penalty factor 3
PF_c by glass cover for glazed portion, a penalty factor
P_{gi} partially saturated vapor pressure of glass cover, in (N/m^2)
Q_{uN} the heat transfer rate to N identical 25% PVT-CPC connected in series, in (kWh)
r_{11} outerdia of helical coiled heat exchanger tube, in (m)
r_{22} innerdia of helical coiled heat exchanger tube, in (m)
T_{giE} eastside, inside glass cover temperature, in $(°C)$
T_{giw} westside, inside glass cover temperature, in $(°C)$
T_{goE} eastside temperature of the outside glass cover, in $(°C)$

T_{goW} westside temperature of the outside glass cover, in $(°C)$
T_a surrounding temperature in(°C)
T_c the temperature of solar cell in(°C)
T_{cN} the average temperature of a solar cell, in (°C)
T_{fi} fluid inlet temperature in (°C)
T_{bf} in collector base fluid temperature, in (°C)
T_{foN} N^{th} collector outlet water temperature in (°C)
T_{nf} nanofluid temperature in(°C)
T_p absorbing plate temperature in (°C)
T_s sun temperature in(°C)
T_v vapor temperature in(°C)
T_w the temperature of basin water in(°C)
T_{wo} temperature of water at t=0, in(°C)
ΔT_{DSSS} temperature between nanofluid and base fluid, in (°C)
ΔT_{CPC} temperature between nanofluid to base fluid at PVT collectors outlet, in (°C)
ΔT_{HE} temperature between nanofluid to base fluid at the heat exchanger, in (°C)
ΔT temperature between T_w and $\frac{T_{giE}}{T_{giW}}$ for time(t), in (h)
U_{ba} sink line to surrounding, coefficient of overall heat transfer, in $(W/m^2\ K)$
U_{ga} condensing cover to surrounding, overall heat transfer coefficient, in $(W/m^2\ K)$
U_{gaE} condensing cover to surrounding, overall heat transfer coefficient eastside, in $(W/m^2\ K)$
U_{gaW} condensing cover to surrounding, overall heat transfer coefficient, in $(W/m^2\ K)$
U_{Lc} glazing to surrounding, overall heat transfer coefficient, in $(W/m^2\ K)$
U_{Lm} module to surrounding, overall heat transfer coefficient, in $(W/m^2\ K)$
U_{tca} solar cell to surrounding, overall heat transfer coefficient, in $(W/m^2\ K)$
U_{tpa} absorbing plate to surrounding, overall heat transfer coefficient, in $W/m^2\ K$
$U_{tc,p}$ solar cell to absorbing plate, overall heat transfer coefficient, in $(W/m^2\ K)$
X characteristic length, solar distiller unit, in (m)

Greek letters

α_g solar energy fraction absorbed by the condensing cover
α_b solar energy fraction absorbed by basin surface
α_f solar energy fraction absorbed by the fluid
α_c solar energy fraction absorbed by solar cell
β packing factor
β_p nanoparticles, coefficient of thermal expansion, in (K^{-1})
β_{nf} nanofluid coefficient of thermal expansion, in (K^{-1})
β_{bf} base fluid coefficient of thermal expansion, in (K^{-1})
$\emptyset_g$ nanoparticles fraction of volume, in (%)
μ_{bf} base fluid viscosity of dynamic, in (Ns/m^2)
μ_{nf} nanofluid viscosity of dynamic, in (Ns/m^2))
η_g collectors efficiency, in %
ρ_p nanoparticles density, in (Kg/m^3)
ρ_{nf} nanofluid density, in (Kg/m^3)
ρ_{bf} base fluids density, in (Kg/m^3)
τ_g transmitted fraction of glass cover

Subscripts

a ambient
a_n per annum
b basin
E eastside
e_n energy
e_x exergy
E_{in} embodied energy input
E_{out} embodied energy output
E_{sol} annual solar energy
f fluid
g_i condensing cover inside
g_o condensing cover outside
i interest rate
n life period
p particle
S_{ol} solar
th thermal
v vapor
W westside

Abbreviation

AMC maintenance costs annually
ASC salvage cost annually
BF base fluid
CRF capital recovery factor
C per liter yield price
CM carbon dioxide mitigation
DS double slope distiller unit
EPT payback time of energy
EPF payback factor of energy
FAC fixed annual cost
FPC collector, flat plate
HE heat exchanger
HTC coefficient of heat transfer
LCCE efficiency of life cycle conversion
NF nanofluid
NP nanoparticle
PCC primary capital cost
PVT photovoltaic thermal
R reflectors
SFF shrinking fund factor
S value of future salvage
TAC total annual cost
CPC compound parabolic concentrator
N-PVT-DS-CPC-HE, incorporating PVT-CPC double slope with N^{th} collector using a heat exchanger (helically coiled)

Appendix A

$$A_1 = C_1U_1 + C_2$$

$$C_1 = \alpha_g I_{SE} A_{gE} + U_{cgaE} A_{gE} T_a$$

$$C_2 = \alpha_g I_{SW} A_{gE} A_{gW} h_{EW} + U_{cgaW} A_{gE} T_a A_{gW} h_{EW}$$

$$U_1 = h_{1wE}\frac{A_b}{2} + h_{Ew}A_{gE} + U_{cgaE}A_{gE}$$

$$A_2 = (h_{1wE}U_2 + h_{1wW}h_{Ew}A_{gE})\frac{A_b}{2}$$

$$U_2 = U_{cgaW}A_{gW} + h_{1wW}\frac{A_b}{2} + h_{Ew}A_{gW}$$

$$B_1 = C_1'U_1 + C_2'$$

$$B_2 = (h_{1wW}U_1 + h_{1wE}h_{Ew}A_{gE})\frac{A_b}{2}$$

$$C_1' = \alpha_g I_{SW} A_{gE} + U_{cgaW} A_{gE} T_a A_{gW}$$

$$C_2' = \alpha_g I_{SE} A_{gE} A_{gW} h_{EW} + U_{cgaE} A_{gE} T_a A_{gW}$$

$$D_1 = m_f C_f (K_m^N - \frac{(1-e^{-z})}{(1-e^{-z}K_p^N)})$$

$$D_2 = [\frac{(AF_R(\alpha\tau))1(1-K_p^N)}{(1-K_p)}\left(1-\frac{e^{-z}}{(1-e^{-z}K_p^N)}\right)]$$

$$D_3 = [\frac{(AF_R(UL)1)(1-K_p^N)}{(1-K_p)}\left(1-\frac{e^{-z}}{(1-e^{-z}K_p^N)}\right)]$$

$$E_1 = U_{gaE}[h_{EW} + h_{1bwW}(\frac{A_b}{2A_{gW}})$$

$$E_1' = U_{gaW}[h_{EW} + h_{1bwE}(\frac{A_b}{2A_{gE}})$$

$$E_2 = U_{gaW}(h_{EW} + U_{gaE})A_{gE}A_{gW}$$

$$E_2' = U_{gaE}(h_{EW} + U_{gaW})A_{gE}A_{gW}$$

$$H_1 = (U_{gaE} + U_{gaW})h_{1bwW}h_{1bwE}(\frac{A_b}{2})$$

$$H_2 = A_{gE}A_{gW}h_{EW}(U_{gaE}h_{1bwE} + U_{gaW}h_{1bwW})$$

$$H_3 = A_{gE}A_{gW}U_{gaE}U_{gaW}(h_{1bwE} + h_{1bwW})$$

$$H_4 = A_{gE}A_{gW}h_{EW}(U_{gaE}h_{1bwW} + U_{gaW}h_{1bwE})$$

$$H_{11}' = H_1 + H_2 + H_3 + H_4$$

$$H_{33}' = U_bA_b - D_1$$

$$H_{44}' == U_bA_b + D_3$$

$$K_{1E} = [h_{1bwW}\left(\frac{A_b}{2A_{gW}}\right) + h_{EW}\left(1+\frac{1}{h_{1bwE}}\right) + U_{gaW}]A_{gW}\alpha_g A_{gE} h_{1bwE}$$

$$K_{1W} = [h_{1bwE}\left(\frac{A_b}{2A_{gE}}\right) + h_{EW}\left(1+\frac{1}{h_{1bwW}}\right) + U_{gaE}]A_{gW}\alpha_g A_{gE} h_{1bwW}$$

$$K_{1E}' = [h_{1bwW}\left(\frac{A_b}{2}\right) + h_{EW}\left(1+\frac{h_{1wE}}{h_{1wW}}\right)A_{gW} + U_{gaW}A_{gW}]\alpha_g A_{gE} h_{1wE}$$

$$K'_{1W} = [h_{1bwE}\left(\frac{A_b}{2}\right) + h_{EW}\left(1+\frac{h_{1wE}}{h_{1wW}}\right)A_{gE} + U_{gaE}A_{gE}]\alpha_g A_{gW} h_{1wW}$$

$$P = U_1U_2 - h_{EW}^2 A_{gE} A_{gW}$$

Expressions for K_k, $(A\,F_R(\alpha\tau))_1$ and $(A\,F_R U_L)_1$ used in Eq. (1) are as follows.

$$K_p = 1 - \frac{(AF_R(UL)1)}{m_f c_f}$$

$$K_m = 1 - \frac{(A_{rm}F_{Rm}(UL)m)}{m_f c_f}$$

$$U_{tca} = \left[\frac{1}{h_o} + \frac{L_g}{K_g}\right]^{-1} ; U_{tcp} = \left[\frac{1}{h_i} + \frac{L_g}{K_g}\right]^{-1} ;$$

$$h_o = 5.7 + 3.8V, \quad Wm^{-2}K^{-1} ; V = 1\ ms^{-1} ; h_i = 5.7,\ Wm^{-2}K^{-1};$$

$$U_{tpa} = \left[\frac{1}{U_{tca}} + \frac{1}{U_{tcp}}\right]^{-1} + \left[\frac{1}{h'_i} + \frac{1}{h_{pf}} + \frac{L_i}{K_i}\right]^{-1};$$

$$h'_i = 2.8 + 3V', \quad Wm^{-2}K^{-1} ;$$

$$U_{L1} = \frac{U_{tcp}U_{tca}}{U_{tcp}+U_{tca}} ; U_{L2} = U_{L1} + U_{tpa} ; U_{Lm} = \frac{h_{pf}U_{L2}}{F'h_{pf}+U_{L2}} ; U_{Lc} = \frac{h_{pf}U_{tpa}}{F'h_{pf}+U_{tpa}} ;$$

$$PF_1 = \frac{U_{tcp}}{U_{tcp} + U_{tca}} ; PF_2 = \frac{h_{pf}}{F'h_{pf} + U_{L2}} ; PF_c = \frac{h_{pf}}{F'h_{pf} + U_{tpa}} ;$$

$$(\alpha\tau)_{1eff} = \rho(\alpha_c - \eta_c)\tau_g\beta_c\frac{A_{am}}{A_{rm}} ; (\alpha\tau)_{2eff} = \rho\alpha_p\tau_g^2(1-\beta_c)\frac{A_{am}}{A_{rm}} ;$$

$$(\alpha\tau)_{meff} = [(\alpha\tau)_{1eff} + PF_1(\alpha\tau)_{2eff}] ; (\alpha\tau)_{ceff} = PF_c.\rho\alpha_p\tau_g\frac{A_{ac}}{A_{rc}} ;$$

$$(AF_R(\alpha\tau))_1 = \left[A_cF_{Rc}(\alpha\tau)_{ceff} + PF_2(\alpha\tau)_{meff}A_mF_{Rm}\left(1 - \frac{A_cF_{Rc}U_{Lc}}{\dot{m}_f c_f}\right)\right] ;$$

$$(AF_RU_L)_1 = \left[A_cF_{Rc}U_{Lc} + A_mF_{Rm}U_{Lm} + A_mF_{Rm}U_{Lm}\left(1 - \frac{A_cF_{Rc}U_{Lc}}{\dot{m}_f c_f}\right)\right]$$

$$A_{rm} = b_r L_{rm} ; A_{am} = b_o L_{am} ;$$

$$A_cF_{Rc} = \frac{\dot{m}_f c_f}{U_{Lc}}\left[1 - \exp\left(\frac{-F'U_{Lc}A_c}{\dot{m}_f c_f}\right)\right] ;$$

$$A_mF_{Rm} = \frac{\dot{m}_f c_f}{U_{Lm}}\left[1 - \exp\left(\frac{-F'U_{Lm}A_m}{\dot{m}_f c_f}\right)\right] ;$$

$$z = \frac{2\pi r_{11} U_L}{\dot{m}_f c_f}$$

CONFLICT OF INTEREST

The authors hereby declare that there is no conflict of interest.

REFERENCES

[1] S. A. Lawrence, G. N. Tiwari, Theoretical evaluation of solar distillation under natural circulation with heat exchanger, Energy Convers. Manage., 30 (1990) 205-13. https://doi.org/10.1016/0196-8904(90)90001-F

[2] C. Popiel, and J. Wojtkowiak, Simple formulas for thermo-physical properties of liquid water for heat transfer calculations (from ° C to 150 °C). Heat Transfer Eng, 19 (1998) 87-101. https://doi.org/10.1080/01457639808939929

[3] B. C. Pak, Y. I. Cho., hydrodynamic and heat transfer study of dispersed fluids with submicron metallic oxide particles. Exp Heat Transfer: A J Therm. Energy Generation, Transport, Storage, Convers 11 (1998) 151-70. https://doi.org/10.1080/08916159808946559

[4] G. N. Tiwari, Solar energy: fundamentals, design, modelling and applications. New Delhi/NewYork: CRC Publication/ Narosa Publishing House; 2002

[5] K. S. Hwang, J. H. Lee, S. P. Jang , buoyancy-driven heat transfer of water-based Al2O3 nanofluids in a rectangular cavity, Int. J. Heat Mass Transfer, 50 (2007) 4003-10.

https://doi.org/10.1016/j.ijheatmasstransfer.2007.01.037
[6] O. O. Barden, Experimental study of the enhancement parameters on a single slope solar still productivity, Desalination, 209 (2007) 136-43. https://doi.org/10.1016/j.desal.2007.04.022
[7] G.N. Tiwari, A. K. Tiwari Solar distillation practice for water desalination systems, New Delhi, Anamaya Publishers, 2008.
[8] C. J. Ho, M. W. Chen, Z. W. Li, numerical simulation of natural convection of nanofluid in a square enclosure: effects due to uncertainties of viscosity and thermal conductivity, Int. J. HeatMass Transfer, 51 (2008) 4506-16. https://doi.org/10.1016/j.ijheatmasstransfer.2007.12.019
[9] T. P. Otanicar, J. Golden, Comparative environmental and economic analysis of conventional and nanofluid solar hot water technologies, Environ Sci. Technol., 43 (2009) 6082-7. https://doi.org/10.1021/es900031j
[10] H. E. Patel, T. Sundararajan, S. K. Das, An experimental investigation into the thermal conductivity enhancement in oxide and metallic nanofluids. J. Nanoparticle Res. 12 (2010) 1015-31. https://doi.org/10.1007/s11051-009-9658-2
[11] P. K. Singh, K. B. Anoop, T. Sundararajan, K. D. Sarit, entropy generation due to flow and heat transfer in nanofluids, Int. J. Heat Mass Transfer, 53 (2010) 4757-67. https://doi.org/10.1016/j.ijheatmasstransfer.2010.06.016
[12] M. G. J. D. Elzen, A. D Hof, A. M. Beltran, G. Grassi, M. Roelfsema, B. V. Ruijven, The Copenhagen accord: abatement costs and carbon prices resulting from the submissions, Environ. Sci. Policy, 14 (2011) 28-39. https://doi.org/10.1016/j.envsci.2010.10.010
[13] K. Khanafer and K. Vafai, A critical synthesis of thermo-physical characteristics of nanofluids, Int. J. Heat Mass Transfer, 54 (2011) 4410-28 https://doi.org/10.1016/j.ijheatmasstransfer.2011.04.048
[14] V. Khullar, H. Tyagi, A study on environmental impact of nanofluid based concentrating solar water heating system, Int J. Environ. Studies, 69 (2012) 220-32 https://doi.org/10.1080/00207233.2012.663227
[15] M. Faizal, R. Saidur, S. Mekhilef, M. A. Alim, Energy, economic and environmental analysis of metal oxides nanofluid for flat-plate solar collector, Energy Convers. Manage., 76 (2013)162-8. https://doi.org/10.1016/j.enconman.2013.07.038
[16] X. Liu, W. Chen, M. Gu, S. Shen, G. Cao, Thermal and economic analyses of solar desalination system with evacuated tubular collectors, Solar Energy, 93 (2013) 144-50. https://doi.org/10.1016/j.solener.2013.03.009
[17] A. E. Kabeel, Z. M. Omara, F. A. Essa, Enhancement of modified solar still integrated with external condenser using nanofluids, an experimental approach. Energy Convers.Manage., 78(2014) 493-8. https://doi.org/10.1016/j.enconman.2013.11.013
[18] T. Elango, A. Kannan, K. K. Murugavel, Performance study on single basin single slope solar still with different water nanofluids, Desalination, 360 (2015) 45-51. https://doi.org/10.1016/j.desal.2015.01.004
[19] Z. M. Omara, A. E. Kabeel, F. A. Essa, Effect of using nanofluids and providing vacuum on the yield of corrugated wick solar still. Energy Convers.Manage., 103 (2015) 965-72. https://doi.org/10.1016/j.enconman.2015.07.035
[20] G.N. Tiwari, J.K. Yadav, D.B. Singh, I.M. Al-Helal, A.M. Abdel-Ghaney, Exergoeconomic and enviroeconomic analyses of partially covered photovoltaic flat plate collector active solar distillation system, Desalination,367(2015) 186-96. https://doi.org/10.1016/j.desal.2015.04.010
[21] H. Sharon, K. S. Reddy, Performance investigation and enviro-economic analysis of active vertical solar distillation units, Energy, 84 (2015) 794-807. https://doi.org/10.1016/j.energy.2015.03.045
[22] L. Sahota, G. N. Tiwari, Effect of Al_2 O_3 NPs on the performance of passive double slope solar still, Solar Energy, 130 (2016) 260-72. https://doi.org/10.1016/j.solener.2016.02.018
[23] D. B. Singh, G. N. Tiwari, I. M. Al-Helal, V. K. Dwivedi, J. K. Yadav, Effect of energy matrices on life cycle cost analysis of passive solar stills, Solar Energy, 134 (2016) 9-22. https://doi.org/10.1016/j.solener.2016.04.039
[24] L. Sahota, G. N. Tiwari, Effect of nanofluids on the performance of passive double slope solar still: A comparative study using characteristic curve. Desalination, 388 (2016) 9-21. https://doi.org/10.1016/j.desal.2016.02.039
[25] D. B. Singh and G. N. Tiwari, Effect of energy matrices on life cycle cost analysis of partially covered photovoltaic compound parabolic concentrator collector active solar distillation system, Desalination, 397 (2016) 75-91. https://doi.org/10.1016/j.desal.2016.06.021
[26] S. W. Sharshir, G. Peng, L. Wu, N. Yang, F. A. Essa, A. H. Elsheikhd, Enhancing the solar still performance using nanofluids and glass cover cooling: Experimental study. Appllied Thermal Engg., 113 (2017) 684-93. https://doi.org/10.1016/j.applthermaleng.2016.11.085
[27] L. Sahota, G. N. Tiwari, Analytical characteristic equation of nanofluid loaded activedouble slope solar still coupled with helically coiled heat exchanger. Energy Convers. Manage., 135(2017) 308-26. https://doi.org/10.1016/j.ijleo.2017.01.063
[28] S. M. Saleha, A. M. Solimanb, M. A. Sharaf, V. Kaled, B. Gadgile, Influence of solvent in the synthesis of nano-structured Z_n O by hydrothermal method and their application in solar-still. J. Environ. Chem. Eng., 5 (2017) 1219-26. https://doi.org/10.1016/j.jece.2017.02.004
[29] W. Chen, C. Zou, X. Li, L. Li, Experimental investigation of S_i C nanofluids for solar distillation system: Stability, optical properties and thermal conductivity with saline water based fluid, International Journal of Heat Mass Transfer, 107 (2017) 264-70. https://doi.org/10.1016/j.ijheatmasstransfer.2016.11.048
[30] O. Mahian, A. Kianifar, S. Z. Heris, D. Wen, A. Z. Sahin, S. Wongwises, Nanofluids effects on the evaporation rate in a solar still equipped with a heat Exchanger. doi: http://dx.doi.org/10.1016/j.nanoen.2017.04.025.
[31] L. Sahota, Shyam, G. N. Tiwari, Energy matrices, enviroeconomic and exergoeconomic analysis of passive double slope solar still with water based nanofluids, Desalination, 409 (2017) 66-79. https://doi.org/10.1016/j.desal.2017.01.012
[32] D. B. Singh, G. N. Tiwari, Enhancement in energy metrics of double slope solar still by incorporating N identical PVT collectors, Solar Energy, 143 (2017) 142-161. https://doi.org/10.1016/j.solener.2016.12.039
[33] P. Joshi and G. N. Tiwari, Effect of cooling condensing cover on the performance of N identical photovoltaic thermal compound parabolic concentrator active solar still: a comparative study, International Journal of Energy and Environmental Engineering, 9 (2018) 473-498.

https://doi.org/10.1007/s40095-018-0276-6
[34] Dharamveer, Samsher, D. B. Singh, A. K. Singh, N. Kumar, Solar Distiller Unit Loaded withNanofluid-A Short Review. Lecture Notes in Mechanical Engineering, Springer, Singapore, (2019) 241-247, https://doi.org/10.1007/978-981-13-6577-5_24. https://doi.org/10.1007/978-981-13-6577-5_24
[35] S Kumar and D. Singh, Energy and exergy analysis of active solar stills using compound parabolic concentrator, International Research Journal of Engineering and Technology (IRJET), 6 (2019) 12.
[36] R. Shanker, D. Singh, D. B. Singh “Performance analysis of C.I. engine using biodiesel fuel by modifying injection timing and injection pressure” International Research Journal of Engineering and Technology (IRJET) 6 (2019) 12.
[37] A. K. Anup and D. Singh, FEA analysis of refrigerator compartment for optimizing thermal efficiency, International Journal of Mechanical and Production Engineering Research and Development, 10 (2020) 3, 3951-3972.
[38] S Kumar and D. Singh, Optimizing thermal behavior of compact heat exchanger, International Journal of Mechanical and Production Engineering Research and Development, 10 (2020) 3, 8113-8130.
[39] G.Zhang, N. D.Kaushika, S. C.Kaushik, R. K.Tomar, Advances in Energy and Built Environment, Springer Science and Business Media LLC, 2020. https://doi.org/10.1007/978-981-13-7557-6
[40] R. Dhivagar, M. Mohanraj, K. Hindouri, Y. Belyayev, Energy, exergy, economic and enviroeconomic (4E) analysis of gravel coarse aggregate sensible heat storage assisted single slope solar still, Journal of Thermal Analysis and Calorimetry, https://doi.org/10.1007/s10973-020-09766-w (2020). https://doi.org/10.1007/s10973-020-09766-w
[41] Dharamveer and Samsher, Comparative analyses energy matrices and enviro-economics for active and passive solar still, materialstoday: proceedings, https://doi.org/10.1016/j.matpr.2020.10.001 (2020). https://doi.org/10.1016/j.matpr.2020.10.001
[42] S. Arora, H. P. Singh, L. Sahota, M. K. Arora, R. Arya, S. Singh, A. Jain, A. Singh, Performance and cost analysis of photovoltaic thermal (PVT)-compound parabolic concentrator (CPC) collector integrated solar still using CNT-water based nanofluids, Desalination, 495 (2020) 114595. https://doi.org/10.1016/j.desal.2020.114595
[43] Dharamveer, Samsher, Anil Kumar, Analytical study of Nth identical photovoltaic thermal (PVT) compound parabolic concentrator (CPC) active double slope solar distiller with helical coiled heat exchanger using CuO Nanoparticles, Desalination and water treatment, 233 (2021) 30-51, https://doi.org/10.5004/dwt.2021.27526 https://doi.org/10.5004/dwt.2021.27526
[44] Dharamveer,Samsher, Anil Kumar, Performance analysis of N-identical PVT-CPC collectors an active single slope solar distiller with a helically coiled heat exchanger using CuO nanoparticles, Water supply, October 2021, SCI-E Index, IWA Publication. I.F 1.275,https://doi.org/10.2166/ws.2021.348 https://doi.org/10.2166/ws.2021.348
[45] M. Kumar and D. Singh, Comparative analysis of single phase microchannel for heat flow Experimental and using CFD, International Journal of Research in Engineering and Science (IJRES), 10 (2022) 03, 44-58.
[46] Subrit and D. Singh, performance and thermal analysis of coal and waste cotton oil liquid obtained by pyrolysis fuel in diesel engine, International Journal of Research in Engineering and Science (IJRES), 10 (2022) 04, 23-31.
[47} A. Shahsavar, P. Talebizadehsardari, M. Arıcı, (2022) Comparative energy, exergy, environmental, exergoeconomic, and enviroeconomic analysis of building integrated photovoltaic/thermal, earth-air heat exchanger, and hybrid systems. Journal of cleaner production. 362: 132510. https://doi.org/10.1016/j.jclepro.2022.132510 https://doi.org/10.1016/j.jclepro.2022.132510